ARTICLE NO. 79-0732R

J80-214

Coupled Rotor/Tower Aeroelastic Analysis of Large Horizontal Axis Wind Turbines

10029
$0001
$0006

William Warmbrodt*
NASA Ames Research Center, Moffett Field, Calif.
and
Peretz Friedmann†
University of California, Los Angeles, Calif.

Formulation of the governing nonlinear equations of motion for the coupled rotor/tower dynamics of a large two-bladed horizontal axis wind turbine (HAWT) is presented. Each blade has elastic flap and lead-lag bending deflections and the supporting tower has bending-bending-torsion deflections. Rotor/tower coupling is accomplished by enforcing dynamic equilibrium between the rotor and the top of the tower. The nonlinear periodic coefficient equations of motion are used to study aeroelastic stability and response of the NASA/DOE 100 kW Mod-O wind turbine. The influence of the flexible tower and nonlinear terms on rotor stability is examined. Isolated rotor blade behavior is compared to the complete coupled rotor/tower system and the basic differences are identified. It is concluded that for high tower stiffness, the aeroelastic response is primarily dependent on isolated rotor forcing, yaw mechanism flexibility, and tower shadow effect. It is also shown that rotor stability can be improved by "tuning" the support system stiffness.

Nomenclature

a	= two-dimensional blade airfoil lift-curve slope
$B(\psi_k)$	= tower shadow blockage factor, ≤ 1
c_{do}	= blade airfoil profile drag coefficient
e	= offset between axis of rotation and cantilevered end of blade, $\bar{e}=e/l$
g	= gravitational constant
h	= distance from pylon support to hub
H	= height of tower
K_T	= factor multiplying both uniform tower bending stiffness and torsional rigidity distributions; for Mod-O, $K_T=1.0$
K_Y	= rotational spring stiffness of pylon yaw mechanism
l	= length of blade capable of elastic deformation, $l=R-e$
M_B, M_P, M_T	= mass of blade, pylon, and tower, respectively
R	= radius of blade
u_g, v_g, w_g	= wind gust velocity components
u_k, v_k, w_k	= blade elastic bending deflections in axial, lead-lag, and flap directions, respectively
v_T, w_T	= tower elastic bending deflections
V_{Gk}	= magnitude of incoming mean gradient wind velocity
V_0	= mean wind velocity at top of tower
x_k	= kth blade radial coordinate along elastic axis
x_T	= tower heightwise coordinate
$\{y\}$	= state variable column vector
$\{\bar{y}\}$	= linear steady-state response vector
α	= constant exponent in gradient wind profile expression
β_P	= blade precone angle with respect to hub plane
ζ_j	= real part of jth characteristic exponent of homogeneous system
η_{SL}, η_{SF}	= blade lag and flap critical damping factors
η_{STX}, η_{STY}, η_{STZ}	= tower critical damping factors
η_{SYM}	= yaw mechanism critical damping factor
θ_0	= collective pitch setting
λ_j	= jth characteristic multiplier
ϕ_P	= yaw mechanism elastic rotation
ϕ_T	= tower elastic torsion deformation
$[\Phi_L(\psi)]$	= transition matrix of linear homogeneous set of equations
ψ_k	= kth blade azimuth angle
ψ_1, ψ_2	= azimuth angles specifying region of tower shadow
ω_F, ω_L, ω_T	= fundamental rotating flap, lag, and torsion frequencies of rotor blade
ω_{TY}, ω_{TZ}, ω_{TX}	= fundamental tower bending and torsion frequencies
Ω	= constant rotor speed of rotation

Superscripts

$(\bar{\ })$	$=(\ )/\Omega$
$(\dot{\ })$	$=d/dt(\ )$
$(*)$	$=d/d\psi_k$, $(\dot{\ })=(*)\Omega$

I. Introduction

LARGE horizontal axis wind turbines (HAWT) used for generating electricity from the wind are sophisticated dynamic systems in which structural dynamic and aeroelastic problems can be frequently encountered. These problems appear due to a combination of factors involving the large rotating structures, their flexibility, and the turbulent atmospheric wind environment in which they operate. Proper analytical modeling of the dynamics of large wind turbines requires the incorporation of a number of system parameters and operating conditions into the mathematical model. The most important of these are the effects of the tower and yaw

Presented as Paper 79-0732 the AIAA/ASME/ASCE/AHS 20th Structures, Structural Dynamics, and Materials Conference, St. Louis, Mo., April 4-6, 1979; submitted Sept. 4, 1979; revision received Jan. 15, 1980. This paper is declared a work of the U.S. Government and therefore is in the public domain.

Index categories: Structural Dynamics; Aeroelasticity and Hydroelasticity; Wind Power.

*Research Scientist. Member AIAA.

†Associate Professor, Mechanics and Structures Department, School of Engineering and Applied Science. Associate Fellow AIAA.

mechanism flexibility (the yaw mechanism is used to align the rotor disk normal to the oncoming mean wind), gradient wind velocity and direction of approach, wind gusts, gravitational loads, and the tower interference effect on air flow through the rotor disk (tower shadow effect) for configurations where the rotor operates behind the tower (downwind rotors).

Recent research on isolated large horizontal axis wind turbine blades[1] has indicated that nonlinear terms, associated with finite blade slopes, can significantly affect the aeroelastic stability of such blades. Consequently, the treatment of this aeroelastic problem requires a careful and relatively consistent derivation of the dynamic equations of equilibrium such that moderate deflections based upon the assumption of small strains and finite slopes are properly incorporated in the mathematical model.

The present paper has a number of objectives: first, to extend the isolated blade analysis, presented in Ref. 1, to the complete coupled rotor/tower dynamic system; second, to present a derivation of the nonlinear equations of motion for coupled rotor/tower dynamics of large horizontal axis wind turbines with an emphasis on the methodology required for the coupling of the rotor to the tower; and third, to illustrate the relative importance of support motion and the operating environment by using the results obtained from a digital computer simulation.

Although the literature on the aeroelastic behavior of large horizontal axis wind turbines is relatively new, a considerable amount of research in this field has recently become available and is reviewed in a recent survey paper.[2] The topic of coupled rotor/tower dynamics has received only limited attention due to its complexity. Since the coupled rotor/tower dynamics of large HAWT's are somewhat similar to helicopter coupled rotor/fuselage systems and tilt prop/rotor systems,[3-9] the methodology established in these studies can be adapted to the HAWT problem provided that some fundamental differences[2,10,11] are carefully incorporated in the analysis.

The aeroelasticity of helicopter rotors in hover and forward flight has been extensively reviewed in Ref. 3. Coupled rotor/support dynamic problems are commonly referred to as aeromechanical problems in rotary wing aeroelasticity. Ground and air resonance of rotors mounted on flexible supports have been investigated, for particular rotor configurations, in Refs. 4-6. Large general purpose computer programs,[7,8] analyze coupled system dynamics and performance of helicopters. Furthermore, the mathematical model of a large prop/rotor mounted on a flexible wing[9] is somewhat similar to the model required to analyze coupled rotor/tower systems.

Recent efforts have been aimed towards adapting this existing technology to the analysis of large HAWT's. Surveys of several aspects of this problem can be found in Refs. 2, 10, and 11. Recent studies have considered the dynamics of isolated HAWT blades using a simple hinged offset rigid blade model,[12] and a fully elastic blade model with flap, lead-lag, and torsional deflections.[1] The flap-lag stability of a simplified three-bladed wind turbine rotor, with the hub fixed in space, was analyzed in Ref. 13. A modified version of the REXOR computer program,[7] capable of analyzing the loads and performance of large wind turbines exists[14]; however, the documentation of this program is incomplete. A computer program[15] with the capability of analyzing the coupled rotor/tower dynamic problems of horizontal axis wind turbines, including the rotor, tower, nacelle, power train, control system, and electrical generating system is also available. In a recent paper, Kaza et al.[16] evaluated the capability of this program. It was found that the code is capable of predicting dynamic loads of two-bladed wind turbines; however, the capability of the program to predict aeroelastic boundaries is questionable. A good summary of recent research done at M.I.T. on the dynamics of horizontal axis wind turbines can be found in Ref. 17.

A brief review of the literature presented above indicates that coupled rotor/tower analyses for HAWT's having the ability to deal with both the aeroelastic response and the aeroelastic stability problem in a completely statisfactory manner are not available. The present paper summarizes such an analysis. First, a relatively consistent derivation of the nonlinear equations of motion governing the dynamics of a large two-bladed HAWT is outlined. Each blade has elastic flap and lead-lag deflections; the tower has two bending deflections, in-plane and out-of-plane of rotor rotation, and torsion. The analysis includes many important effects that characterize a wind turbine configuration (as opposed to helicopter rotors): gradient mean wind velocity due to atmospheric boundary layer, gusts, nonalignment between wind and rotor axis, high inflow aerodynamics, gravitational effects, tower shadow effect, and yaw mechanism flexibility. The model takes advantage of the fact that wind turbine blades are structurally much stiffer than helicopter rotor blades. Results are presented to illustrate the importance of these effects on both the aeroelastic stability and aeroelastic response characteristics of the NASA/DOE 100 kW Mod-C experimental wind turbine.[18,19]

II. Formulation of the Problem

A. General

The two-bladed HAWT rotor/pylon/tower model is shown in Fig. 1. The rotor has two blades with distributed mass and stiffness properties. Each blade can have out-of-plane w_k and inplane bending v_k. The blades are assumed to be torsionally rigid. This assumption is justified because typical HAWT blades are very stiff in torsion, $\bar{\omega}_T \cong 10\bar{\omega}_F$. Results presented in the paper and in Ref. 1 show that for the Mod-O machine this assumption is not restrictive. The supporting tower has distributed mass and stiffness properties and can deform in bending-bending-torsion. The pylon is rigidly attached to the supporting tower except for the flexible yaw mechanism (Fig. 1). The yaw mechanism is modeled as a linear torsional spring and viscous damper.

B. Mathematical Model

The rotor mathematical model used in this analysis is identical to the isolated blade model of Ref. 1 except that the blades are assumed to be torsionally rigid. This assumption is shown to be nonrestrictive for the rotor analyzed herein.

The tower is modeled as a tapered cantilever beam. The pylon is assumed to be rigidly attached to the supporting tower except for the flexible yaw mechanism. No electrical generator dynamics are modeled. For further detail the interested reader is directed to Refs. 21 and 22.

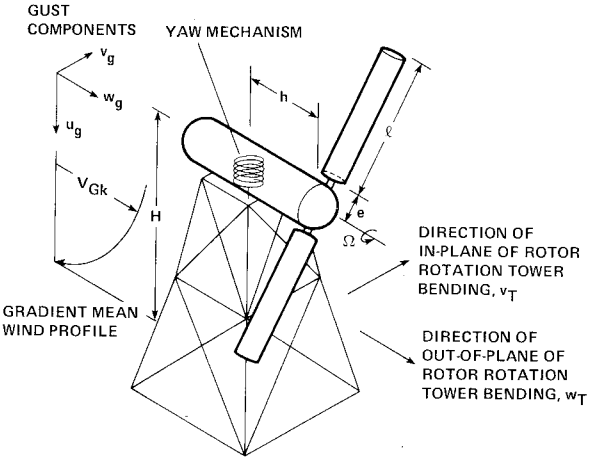

Fig. 1 Wind turbine model.

C. Ordering Scheme

In the process of deriving governing nonlinear differential equations, a considerable number of terms that may be small and negligible are encountered. To neglect higher order terms in a systematic manner, an ordering scheme is used. All quantities are assigned an order of magnitude in terms of a nondimensional quantity ϵ which represents typical elastic blade slopes. The ordering scheme is then used with the assumption that terms of $O(\epsilon^2)$ are negligible when compared to terms of order one, i.e., $1+O(\epsilon^2)\cong 1$. The assigned orders of magnitude of the more important quantities used in this study are:

$$\frac{\partial}{\partial x_T},\ \frac{\partial}{\partial x_k},\ \frac{\partial}{\partial \psi_k},\ \frac{R}{H},\ \frac{l}{H}=O(1)$$

$$\frac{V_{Gk}}{\Omega R},\ \frac{h}{l}=O(\epsilon^{1/2});\quad \frac{v_k}{l},\ \frac{w_k}{l},\ \frac{e}{l}=O(\epsilon)$$

$$\frac{v_T}{H},\ \frac{w_T}{H},\ \phi_T,\ \phi_P,\ \frac{u_g}{\Omega R},\ \frac{v_g}{\Omega R},\ \frac{w_g}{\Omega R},\ \frac{g}{\Omega^2 l}=O(\epsilon^{3/2})$$

$$\frac{u_k}{l},\ \frac{c_{do}}{a}\doteq O(\epsilon^2)$$

The assignment of support deflections and rotations as $O(\epsilon^{3/2})$ implies a stiff supporting tower. The systematic application of this ordering scheme in the derivation procedure will yield a relatively accurate set of nonlinear equations of motion.

III. Blade Equations of Motion

The governing equations of motion for the kth blade, $k=1,2$, with lead-lag and flap deflections are taken from Ref. 20 and also appear as Eqs. (1-3) of Ref. 1.

The distributed loading terms in these equations include inertia, aerodynamic, gravitational, and viscous structural damping effects. To determine the aerodynamic loads, the inclusion of the atmospheric gradient wind, the tower shadow effect, and the high inflow effect (required for the calculation of the airfoil hub plane force) are handled in a manner identical to Ref. 1.

The kth blade equations of motion for the lead-lag and flap deflections are algebraically very long and are not presented here. The equations do appear in Ref. 21. The complete rotor is presented by a system of four second-order nonlinear partial differential equations with periodic coefficients.

It is important to note that this set of equations is written in the rotating, undeformed blade coordinate directions. No transformation to nonrotating hub-fixed (multiblade) coordinates is made. For a two-bladed rotor experiencing azimuth-dependent aerodynamic and inertia loads, multiblade coordinates would not remove the periodic coefficients from the governing equations. Consequently, the rotor blade deflections remain defined in the rotating blade-fixed reference system.

IV. Tower Equations of Motion and Matching Conditions

In the previous section the derivation of the governing lead-lag and flap equations of motion for the kth blade, $k=1,2$, was briefly discussed. The inertia, aerodynamic, gravitational, and damping loads are functions of blade and support deformations. The rotor equations are coupled to the tower through the forcing terms in the loading expressions.

The governing equations of motion for tower bending-bending-torsion are taken from Euler-Bernoulli beam theory. The distributed tower loads include inertia effects and profile drag forces. At the base of the tower the boundary conditions are those of a built-in beam. The boundary conditions at the tower/pylon junction are a statement of moment and force equilibrium between tower elastic deformations, taken from elementary beam theory, and the forces and moments induced by the rotor and pylon.

The rotor-induced forces and moments are calculated by first considering the individual blade distributed force and moment expressions. The net effect of these loads is to transfer to the hub three resultant forces and three resultant moments in a reference system rotating with the blade. Transforming these loads into a hub-fixed nonrotating system and summing the individual components of both blades yield the net rotor hub forces and moments. Likewise, the pylon induces inertial forces and moments at the top of the tower. Complete expressions for the loads can be found in Ref. 21. To restrict the tremendous number of terms and yet retain a valid analytical model, rotor aerodynamic terms of $O(\epsilon^{3/2})$ and higher in the rotor-induced forces and moments were neglected. This is a restrictive assumption on the coupled system analysis and should be kept in mind when interpreting results presented herein.

V. System Equations of Motion

The final system of equations includes elastic flap and lead-lag motion for each blade, the three tower equations of motion, the yaw mechanism equation, and the five natural boundary conditions at the top of the tower.

To solve this set of equations the extended Galerkin method[23] is applied. In doing so, the tower natural boundary conditions are incorporated into the tower equations of motion by combining the boundary-condition residuals with the appropriate differential-equation residual. A transformation to first-order state variable form is then made. This finally yields a set of ordinary first-order nonlinear differential equations with periodic coefficients. These equations are given in Ref. 21.

VI. Method of Solution

The final system of equations may be written in the form

$$\{\overset{*}{y}(\psi)\}=[E(\psi)]\{y\}+\{G(\psi)\}+\{H(y,\overset{*}{y},\psi)\} \tag{1}$$

Linear aeroelastic stability is studied by considering the linear homogeneous system of periodic coefficient equations.

$$\{\overset{*}{y}_L(\psi)\}=[E(\psi)]\{y_L(\psi)\} \tag{2}$$

Linear system stability is studied by applying Floquet Theory and determining the associated transition matrix at the end of one period, $[\Phi_L(2\pi)]$. Evaluating its characteristic multipliers λ_j and determining whether $|\lambda_j|<1$, for all j, indicates system stability. Nonlinear effects on aeroelastic stability are determined approximately by linearizing the complete nonlinear set of equations about an appropriate time-dependent equilibrium position and again evaluating the eigenvalues of the corresponding transition matrix at the end of one period.

The time-dependent equilibrium position, $\{\bar{y}(\psi)\}$, is calculated from the linear system by determining the initial conditions, $\{\bar{y}(0)\}$, for time-history integration to yield a periodic response.[1]

$$\{\bar{y}(0)\}=\{[I]-[\Phi_L(2\pi)]\}^{-1}[\Phi_L(2\pi)]\cdot\int_0^{2\pi}[\Phi_L(s)]^{-1}\{G(s)\}\,ds \tag{3}$$

Numerical integration of the linear system over one period using $\{\bar{y}(0)\}$ yields $\{\bar{y}(\psi)\}$ which is assumed to be an adequate approximation for the periodic solution to the nonlinear equations. This assumption is valid considering the very minor differences between the linear and complete

nonlinear response presented in Fig. 6. Further justification is given in Ref. 1 (pp. 1386-1388). This periodic steady-state response is then used as the time-dependent equilibrium position about which the nonlinear set of equations is linearized to determine linearized aeroelastic stability. Aeroelastic response is determined by numerically integrating the nonlinear set of equations using the initial conditions of the linear periodic response calculation.

VII. Results and Discussion

Numerical results illustrating the effects of rotor support flexibility on rotor aeroelastic stability and response are presented. The baseline configuration of the blade and tower is the Mod-O 100 kW horizontal axis wind turbine.[18,19] Uniform tower mass and stiffness distributions were selected to yield the experimentally measured fundamental tower bending and torsion frequencies.[19] One uncoupled rotating mode was used to represent each blade flap and lead-lag deflection and tower bending-bending-torsion deflection. For the results presented, the blade rotating frequencies were calculated to be $\bar{\omega}_F = 2.90$ and $\bar{\omega}_L = 4.36$. The tower frequencies were calculated to be $\bar{\omega}_{TX} = 11.63$ and $\bar{\omega}_{TY} = \bar{\omega}_{TZ} = 3.96$. The following quantities were used to model the Mod-O configuration: $l = 17.8$ m, $R = 19.0$ m, $H = 30.5$ m, $h = 3.3$ m, $\bar{e} = 0.0684$, $\Omega = 40$ rpm, $\beta_p = 7$ deg, $K_Y = 3.31 \times 10^7$ N-m/rad, $M_p = 13{,}600$ kg, $M_B = 900$ kg, $M_T = 25{,}400$ kg, $a = 2\pi$, $c_{do} = 0.010$, $\alpha = 0.15$, $\eta_{SL} = \eta_{SF} = 0.0$, $\eta_{STX} = \eta_{SYM} = 0.00025$ and $\eta_{STY} = \eta_{STZ} = 0.02$. Wind gusts were assumed to be zero.

Aeroelastic stability is studied by plotting the real part of the characteristic exponents ζ_j of the system degrees-of-freedom vs the gradient mean wind velocity, $V_0/\Omega R$. The system is stable if $\zeta_j < 0$ for all j. Figure 2 shows the effect of varying the mean wind velocity when the collective pitch setting θ_0 is zero and the flexibility of the yaw mechanism is locked out. The Mod-O machine is designed to produce 100 kW electrical power at $V_0/\Omega R = 0.1$ with $\theta_0 = 0$. For wind velocities other than design speed, θ_0 is changed so that the rotor still produces the required torque to give a constant electrical power output of 100 kW. Since $\theta_0 = 0$ in Fig. 2, all the operating states other than $V_0/\Omega R = 0.1$ are off-design operating conditions. Figure 2 shows the rotor flapping modes to be very stable. Tower bending in-the-plane and out-of-the-plane of rotor rotation are both less stable than the tower torsion degree-of-freedom. The characteristic exponents of each of these degrees-of-freedom are insensitive to variation of the mean wind velocity V_0. Nonlinear effects on the stability values of these degrees-of-freedom are negligible and only linear values are plotted. The rotor lag modes are less stable and are shown in Fig. 2b for the same operating conditions as Fig. 2a. In this plot, both linear and linearized stability values are shown . The linearized system is considerably less stable than the linear system. For $V_0/\Omega R > 0.1$, nonlinear effects increase in importance. Also shown in Fig. 2b is the real part of the characteristic exponent in lag for an isolated wind turbine with flap-lag deflections. This is a special restricted case of the present coupled rotor/tower analysis. Note that the isolated blade is less stable than either rotor lag mode of the complete HAWT system. Hence, in this case, support flexibility is stabilizing. The trends of the isolated blade stability are the same as the coupled system. Again nonlinear effects are destabilizing. Additionally, as $V_0/\Omega R$ increases, the destabilizing influence of support motion on lag mode stability increases relative to the isolated blade case. It is also important to note that the decoupled isolated flap-lag stability of the Mod-O blade in the present analysis gives excellent agreement with the isolated flap-lag-torsion blade analysis of Ref. 1. This justifies neglecting blade torsion for stability calculations of the Mod-O machine.

Figure 3 shows the linear and linearized first rotor lag mode stability values when the rotor is trimmed to produce a constant power output. Details of the trim calculation required to achieve the constant power operating state can be

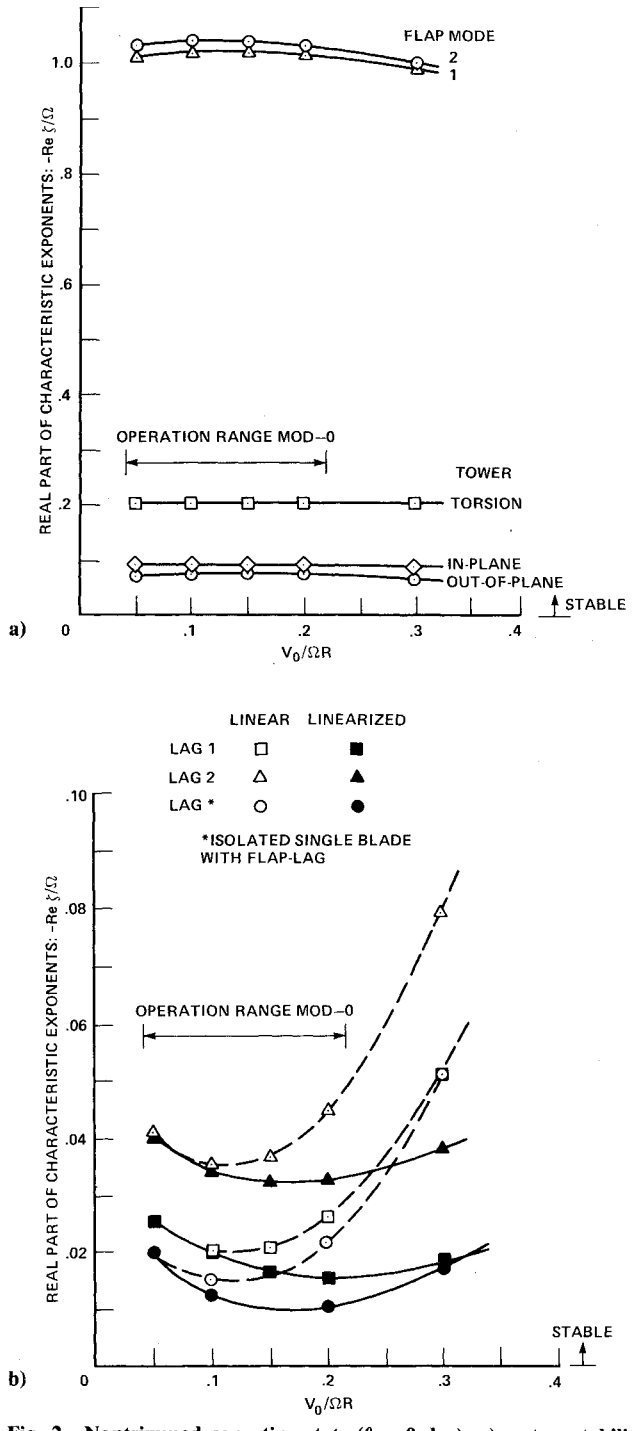

Fig. 2 Nontrimmed operating state ($\theta_0 = 0$ deg); a) system stability and b) rotor lag mode stability.

found in the detailed version of Ref. 1. The yaw mechanism flexibility is again locked out. The linearized system stability is seen to be less stable than the linear system with the difference being greatest for small values of V_0. Also plotted in Fig. 3 are again the linear and linearized lag stability values for a single decoupled isolated trimmed blade with flap-lag degrees-of-freedom. Although one lag mode is more stable than the isolated blade, the other lag mode is less stable for most values of V_0. This difference increases as $V_0/\Omega R$ increases above 0.15. Hence, in this case for the first rotor lag mode, support flexibility is generally destabilizing. It is important to note that at $V_0/\Omega R = 0.05$, the linearized lag stability is only 25% of the corresponding linear stability value for the first rotor lag mode.

Figure 4 shows how system stability varies when the rotor is trimmed and the yaw mechanism flexibility is included. The

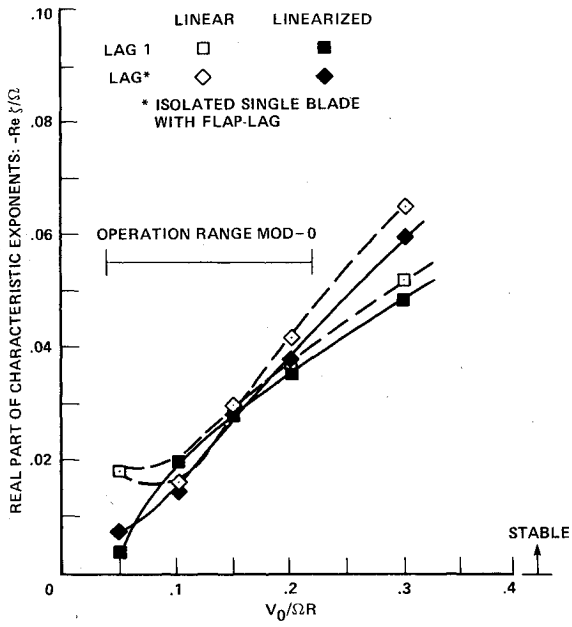

Fig. 3 Trimmed operating state; first rotor lag mode stability.

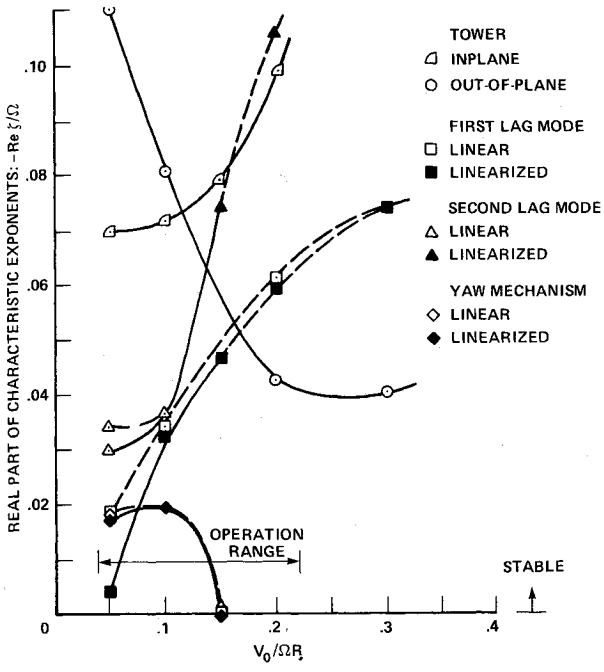

Fig. 4 Trimmed operating state; system stability.

rotor flap and tower torsion modes remain unchanged from Fig. 2a and are not shown. The tower out-of-plane of rotor rotation bending now shows a decrease in stability as V_0 increases. The nonlinear effects on tower bending stability are negligible and are not shown. From the figure it is apparent the rotor lag modes have become more stable than for the trimmed case when the yaw mechanism is locked out. The instability of the yaw mechanism for $V_0/\Omega R = 0.15$ occurs within the operating range of the Mod-O machine. However, if the damping associated with the yaw mechanism spring η_{SYM} were to be increased to 0.0004 this instability is removed from the Mod-O operating range. This very weak instability reflects the importance of the yaw mechanism flexibility on overall system aeroelastic behavior.

The influence of support flexibility on rotor stability is studied in Fig. 5. The linearized stability values for the least stable rotor lag mode are plotted vs mean wind V_0 while

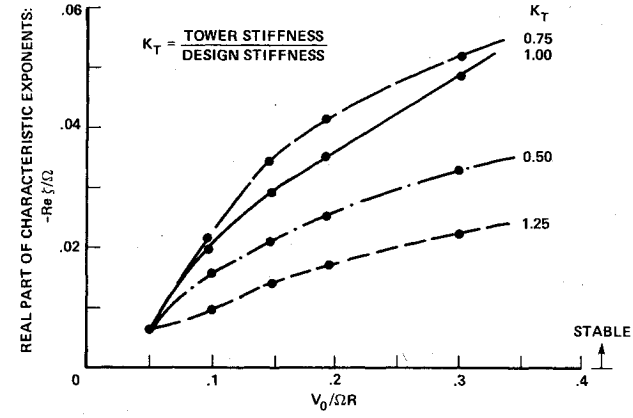

Fig. 5 Influence of support flexibility on linearized stability of first rotor lag mode (trimmed state).

varying tower flexibility. The yaw mechanism is locked out and the rotor is trimmed. Several cases are considered where both the tower uniform bending stiffness and torsional rigidity are varied by a factor K_T. Cases considered include $K_T = 1.25$, 0.75, and 0.50. The calculated tower natural frequencies for these values of K_T are given in Table 1. In Fig. 5, an increase in the supporting system stiffness, $K_T = 1.25$, is dramatically destabilizing for the first lag mode. This is probably due to the tower inplane bending frequency, $\bar{\omega}_{TY} = 4.43$, being very close to the blade inplane bending frequency, $\bar{\omega}_L = 4.36$. Increasing the tower flexibility, $K_T = 0.75$, stabilizes the rotor for all values of V_0. A further increase in tower flexibility, $K_T = 0.50$, destabilizes the rotor lag mode with respect to the actual configuration. This may in part be attributed to the tower bending frequencies, $\bar{\omega}_{TY} = \bar{\omega}_{TZ} = 2.80$, being very close to the blade flap frequency, $\bar{\omega}_F = 2.90$. It is apparent that support flexibility is very important in determining rotor stability. Individual components of the system should be carefully selected to avoid resonances. Most important, even when component frequencies seem well separated, i.e., $K_T = 1.0$, support system "tuning" may result in significant improvements in rotor stability.

Response of the system operating at design conditions with no tower shadow effect is shown in Fig. 6. The generalized coordinate values are plotted for mode shapes normalized to unit deflections at the free ends. Blade 1 bending, yaw mechanism rotation, and tower bending out-of-plane of rotor rotation are shown. Blade 1 is initially located vertically down behind the tower, $\psi = 0$, and rotates to be vertically up at $\psi = 180$ deg. The response of the second blade is the same as shown in Fig. 6 for blade 1 except there exists a phase difference of 180 deg. The flap response reflects the gradient wind variation. There is also a slight phase lag between the minimum wind velocity and the minimum flap response. The lag response shows the influence of both the inplane gravity load as the blade rotates around the azimuth and the inplane aerodynamic force which causes the blade to rotate. The high frequency motion in the rotor response is due to coupling with the yaw mechanism. When the yaw mechanism is locked out,

Table 1 Variations in tower frequencies with K_T; $\bar{\omega}_L = 4.36$ and $\bar{\omega}_F = 2.90$

Tower stiffness coefficient, K_T	Nondimensional tower frequencies	
	Torsion, $\bar{\omega}_{TX}$	Bending, $\bar{\omega}_{TY} = \bar{\omega}_{TZ}$
1.25	13.00	4.43
1.00 (Design)	11.63	3.96
0.75	10.07	3.43
0.50	8.22	2.80

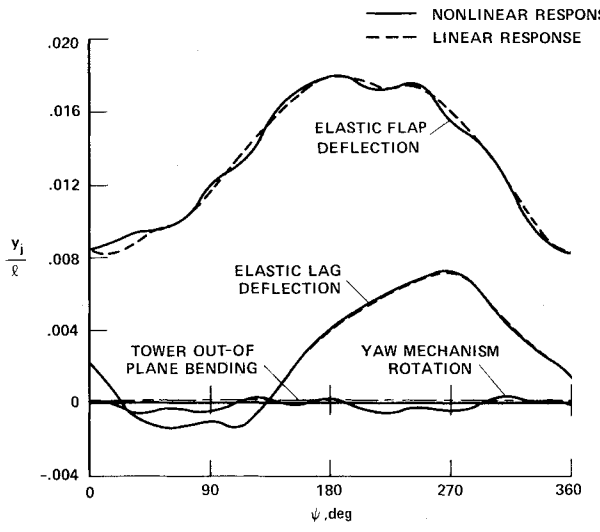

Fig. 6 System response at design conditions ($V_0/\Omega R = 0.10$, $\theta_0 = 0$ deg).

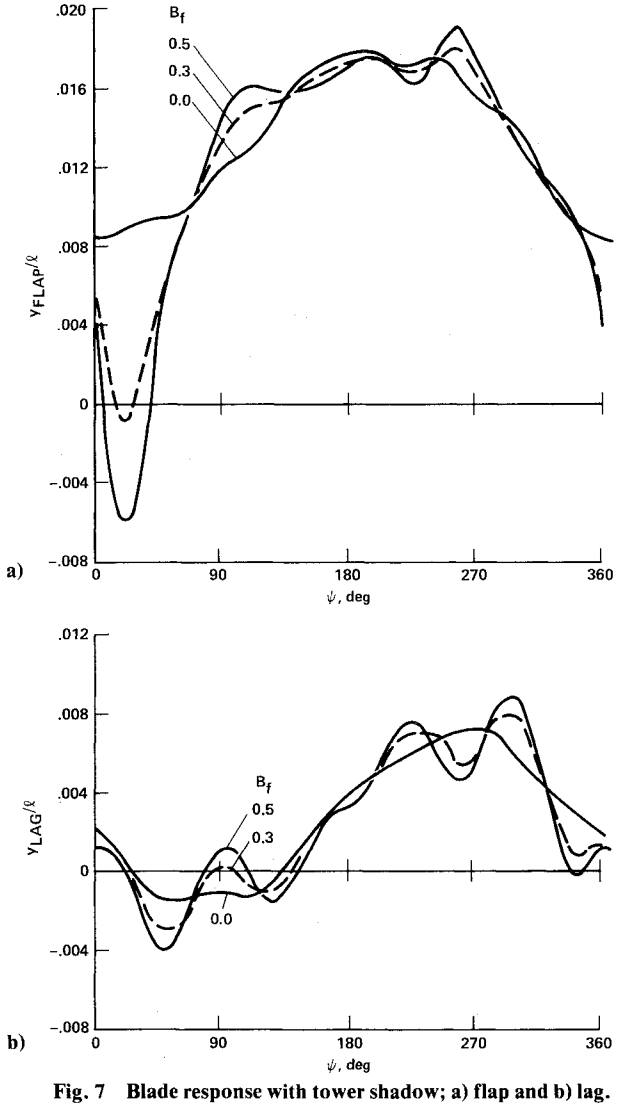

Fig. 7 Blade response with tower shadow; a) flap and b) lag.

this high frequency motion does not appear. Consequently, tower motion does not dramatically influence rotor response due to the large Mod-O tower stiffness. Also shown in Fig. 6 is the linear response of blade 1. It is apparent that although nonlinear effects on rotor stability are important, as seen in Figs. 2b and 3, the influence of nonlinear terms on rotor response is very small for this configuration.

In Ref. 22, the response of an isolated blade with flap-lag deflections, using a restricted set of equations from this analysis, is shown to be almost identical to coupled rotor/tower blade response when the yaw mechanism is locked out. Therefore blade response is due to isolated rotor forcing and yaw mechanism flexibility for the Mod-O configuration. In addition, the isolated flap-lag blade response is very similar to the aeroelastic response of a similar isolated blade with flap-lag-torsion deflections given in Ref. 1. Hence the assumption of a torsionally rigid blade for this configuration is valid for aeroelastic response calculations as well.

The influence of the tower shadow on blade 1 response is shown in Fig. 7 for the design operating condition. The tower blockage was modeled by

$$V_{Gk} = B(\psi_k)\,|V_{Gk}| \tag{4}$$

where

$$B(\psi_k) = \begin{cases} 1 - B_f(1+\cos 12\psi_k), & -15 \text{ deg} < \psi_k < 15 \text{ deg} \\ 1, & 15 \text{ deg} < \psi_k < 345 \text{ deg} \end{cases} \tag{5}$$

Figure 7 shows plots for $B_f = 0$ (no tower shadow), 0.3, and 0.5. The tower shadow is seen to dramatically influence both flap, Fig. 7a, and lag, Fig. 7b, deflections. The large high frequency motion for $\psi > 180$ deg is due to the rotor coupling with the yaw mechanism and is not obtainable from isolated blade analyses. Despite the large influence of the tower shadow on rotor response, it was found to have little influence on rotor stability.

VIII. Conclusions

This paper discusses the formulation of the governing equations of motion of a coupled rotor/pylon/tower system. From the numerical results presented in this paper it is concluded for the two-bladed NASA/DOE Mod-O 100 kW wind turbine, under the restrictions imposed by the analysis, that

1) Support degrees-of-freedom do influence rotor stability and can be stabilizing or destabilizing, depending on operating conditions.

2) Nonlinear effects are important in determining rotor lag stability.

3) The overall system is aeroelastically stable if the yaw mechanism damping is sufficient.

4) Assuming the rotor blades to be torsionally rigid is valid for the configuration studied.

5) Due to the high tower stiffness, the aeroelastic response of the system is primarily dependent on isolated rotor forcing, yaw mechanism flexibility, and tower shadow effect.

6) Although nonlinear terms are important in determining rotor stability, these terms are of lesser importance in evaluating aeroelastic response.

7) Rotor stability can be improved by tuning the support system stiffness. Future designs of large HAWT's should take advantage of this feature to improve aeroelastic behavior.

Acknowledgments

This research was supported by NASA Lewis Research Center, Cleveland, Ohio, under NASA Grant NSG 3082 and was partially funded by AVRADCOM Structures Laboratory and NASA Langley Research Center under NASA Grant 05-007-414.

References

[1] Kottapalli, S.B.R., Friedmann, P., and Rosen, A., "Aeroelastic Stability and Response of Horizontal Axis Wind Turbine Blades,"

AIAA Journal, Vol. 17, Dec. 1979, pp. 1381-1389; a more complete version is also available as University of California School of Engineering and Applied Science Rept. UCLA-ENG-7880, Aug. 1978.

[2] Friedmann, P., "Aeroelastic Stability and Response Analysis of Large Horizontal Axis Wind Turbines," *Journal of Industrial Aerodynamics,* Vol. V, May 1980, pp. 373-401.

[3] Friedmann, P., "Recent Developments in Rotary-Wing Aeroelasticity," *Journal of Aircraft,* Vol. 14, Nov. 1977, pp. 1027-1041.

[4] Coleman, R. P. and Feingold, A. M., "Theory of Ground Vibrations of a Two-Bladed Helicopter on Anisotropic Supports," NACA TN 1184, 1947.

[5] Ormiston, R. A., "Aeromechanical Stability of Soft Inplane Hingeless Rotor Helicopters," *Proceedings of the Third European Rotorcraft and Power Lift Aircraft Forum,* Aix-en-Provence, France, Sept. 1977, pp. 25.1-25.22.

[6] Hodges, D. H., "Aeromechanical Stability of Helicopters with a Bearingless Main Rotor—Part I: Equations of Motion," NASA TM-78459, Feb. 1978.

[7] Anderson, W. D., Connor, F., Kretsinger, P., and Reaser, J. S., "REXOR Rotorcraft Simulation," USAAMRDL-TR-76-28A, July 1976.

[8] McLarty, T. T., "Rotorcraft Flight Simulation with Coupled Rotor Aeroelastic Stability Analysis," USAAMRDL-TR-76-41A, May 1977.

[9] Johnson, W., "Dynamics of Tilting Proprotor Aircraft in Cruise Flight," NASA TN D-7677, May 1974.

[10] Ormiston, R. A., "Dynamic Response of Wind Turbine Rotor Systems," AHS Preprint S-993, presented at the 31st Annual National Forum of the American Helicopter Society, Washington, D.C., May 1975.

[11] Friedmann P., "Aeroelastic Modeling of Large Wind Turbines," *Journal of the American Helicopter Society,* Oct. 1976, pp. 17-27.

[12] Chopra, I. and Dugundi, J., "Nonlinear Dynamic Response of a Wind Turbine Blade," *Journal of Sound and Vibration,* Vol. 63, Jan. 1979, pp. 265-286.

[13] Kaza, K.R.V. and Hammond, C. E., "An Investigation of Flap-Lag Stability of Wind Turbine Rotors in the Presence of Velocity Gradients and Helicopter Rotors in Forward Flight," *Proceedings of the AIAA/ASME/SAE 17th Structures, Structural Dynamics, and Materials Conference,* Valley Forge, Pa., May 1976.

[14] Linscott, B. S., Glasgow, J., Anderson, W. D., and Donham, R. E., "Experimental Data and Theoretical Analysis of an Operating 100 kW Wind Turbine," paper presented at the Twelfth Intersociety Energy Conversion Engineering Conference, Washington, D.C., Aug., 1977.

[15] Hoffman, J.A., "Coupled Dynamic Analysis of Wind Energy Systems," NASA CR-135152, Feb. 1977.

[16] Kaza, K.R.V., Janetzke, D. C., and Sullivan, T. L., "Evaluation of MOSTAS Computer Code for Predicting Dynamic Loads in Two-Bladed Wind Turbines," *Proceedings of the AIAA 20th Structures, Structural Dynamics and Materials Conference,* AIAA Paper 79-0733, St. Louis, Mo., April 1979.

[17] Miller, R. H., Dugundi, J., Chopra, I., Shew, D., and Wendell, J., "Wind Energy Conversion, Vol. 2: Dynamics of Horizontal Axis Wind Turbines," Massachusetts Institute of Technology, Aeroelastic and Structures Research Lab. Rept. ASRL-TR-184-9, Sept. 1978.

[18] Cherritt, A. W. and Gaidelis, J. A., "100 kW Metal Wind Turbine Blade Basic Data, Loads, and Stress Analysis," NASA CR-134956, June 1975.

[19] Chamis, C. C. and Sullivan, T. L., "Free Vibrations of the ERDA-NASA 100 kW Wind Turbine," NASA TMX-71,879, 1976.

[20] Rosen, A. and Friedmann, P., "Nonlinear Equations of Equilibrium for Elastic Helicopter or Wind Turbine Blades Undergoing Moderate Deformation," DOE/NASA/3082-7811, Dec. 1978; also available as NASA CR-159478.

[21] Warmbrodt, W., "Aeroelastic Response and Stability of a Coupled Rotor/Support System with Application to Large Horizontal Axis Wind Turbines," Ph.D. Thesis, Mechanics and Structures Department, University of California, Los Angeles, Aug. 1978; also available as Warmbrodt, W. and Friedmann, P., UCLA-ENG-7881, Aug. 1978.

[22] Warmbrodt, W. and Friedmann, P., "Formulation of the Aeroelastic Stability and Response Problem of Coupled Rotor/Support Systems," *Proceedings of the AIAA/ASME/ASCE/AHS 20th Structures, Structural Dynamics, and Materials Conference,* AIAA Paper 79-0732, St. Louis, Mo., April 1979.

[23] Finlayson, B. A. and Scriven, L. E., "The Method of Weighted Residuals—A Review," *Applied Mechanics Review,* Vol. 19, Sept. 1966, pp. 735-748.